International Food Research Journal 26(5): 1447-1457 (October 2019)

Journal homepage: *http://www.ifrj.upm.edu.my*

The influence of two solvent extraction ratios in GC-MS-based metabolomics of different *Garcinia mangostana* Linn. fruit tissues

Mamat, S. F., Azizan, K. A., Baharum, S. N., Mohd Noor, N. and *Aizat, W. M.

Institute of Systems Biology (INBIOSIS), Universiti Kebangsaan Malaysia (UKM), 43600 Bangi, Selangor, Malaysia

Article history

Received: 10 March, 2019
Received in revised form: 21 June, 2019
Accepted: 31 July, 2019

Keywords

Extraction
GC-MS
Mangosteen
Metabolite
Metabolomics
Multivariate analysis

Abstract

Mangosteen (*Garcinia mangostana* Linn.) is a highly beneficial fruit, containing potent bioactive compounds such as xanthones. However, the metabolite comparisons of mangosteen pericarp, aril and seed have not been described in detail previously. A comparative approach was undertaken in the present work to evaluate the effects of different ratios of solvent combination in the metabolite extraction of mangosteen. Gas chromatography-based metabolomics approach was performed to evaluate the efficiency of two metabolite extraction methods utilising different solvent extraction ratios (3/1/1 v/v or 2/1/2 v/v of methanol/chloroform/water) in determining the primary metabolite composition of mangosteen fruit tissues (pericarp, aril and seed). Cumulatively, 43 known metabolites were putatively identified from the mangosteen fruit tissues. Due to the higher ratio of polar solvent (methanol and water) used in method 2 as compared to method 1, the former method preferentially extracted a higher number of polar metabolites. Conversely, the higher ratio of methanol solvent in method 1 also contributed to the identification of more alcohol metabolites. Additionally, the multivariate analysis revealed that mangosteen pericarp was mainly localised by ribonic acid, arabinopyranose, β-hydroxypyruvic acid, L-(+)-tartaric acid and galacturonic acid. Meanwhile, thymol-α-D-glucopyranoside and D-ribofuranose contributed to the separation of mangosteen aril, whereas mangosteen seed contained high levels of β-D-galactofuranose, L-threonic acid, butanoic acid, glycoside, malic acid and myo-inositol. Results suggested that the differing solvent ratios can highly influence the types and levels of the extracted metabolites. This finding highlights the influence of metabolite solvent extraction methods towards the end results of the extraction as well as the localisation of primary metabolites in different mangosteen fruit tissues. Hence, the present work is vital in revealing important spatial information of various metabolites toward a better understanding of the mangosteen fruit ripening process.

Introduction

Mangosteen (*Garcinia mangostana* Linn.), dubbed as "the queen of fruits", is a tropical fruit native to South East Asian countries (Osman and Milan, 2006). Mangosteen fruit possesses a dark purple outer pericarp with white juicy and refreshing aril inside, and is consumed for both its unique flavour and nutrient content. Various bioactive compounds have been isolated and characterised in mangosteen, particularly xanthones, triterpenes and benzophenones (Jamil *et al*., 2018; Aizat *et al*., 2019). Some of these bioactive compounds possess anti-oxidant (Mohamed *et al*., 2014; Thong *et al*., 2015), anti-inflammatory (Chen *et al*., 2008), anti-malaria (Chaijaroenkul *et al*., 2014) and promising anti-cancer properties (Matsumoto *et al*., 2003; Shibata *et al*., 2011). Due to these medicinal properties, mangosteen has been used in folk medicines and various supplemental products to relieve diarrhoea as well as to treat skin infections, wounds, gonorrhoea, ulcer, abdominal pain and suppuration (Shibata *et al*., 2011; Chaijaroenkul *et al*., 2014; Mohamed *et al*., 2014).

These potential health benefits have made mangosteen a very interesting model organism for the investigation of secondary metabolites. Several studies have focused on the phenolic and xanthone content in this exotic fruit (Zadernowski *et al*., 2009; Sukatta *et al*., 2013). However, only

*Corresponding author.
Email: wma@ukm.edu.my

a few studies have focused on the variations of metabolite composition during the ripening process (Parijadi *et al*., 2018; Mamat *et al*., 2018a; 2018b). Particularly, the composition of primary metabolites in the mangosteen fruit has not been previously emphasised. Primary metabolites may determine the colour, taste, smell, nutritional quality and bioactive properties of a fruit (Osorio *et al*., 2013). Hence, their localisation in different tissues of mangosteen fruit is vital in determining the fruit's metabolic processes.

Metabolite extraction is also an important step in metabolite profiling. Variations in metabolite extraction protocols or sample/tissue types will have significant impacts on the metabolites that can be detected (De Vos *et al*., 2007; Cevallos-Cevallos *et al*., 2009; Mushtaq *et al*., 2014). Several studies have reported such findings using a single extraction method to compare various tissue types (Osorio *et al*., 2013; Vondras *et al*., 2017) and vice versa (comparing different extraction methods using one single tissue) (Gullberg *et al*., 2004; Dettmer *et al*., 2011; Azizan *et al*., 2015). Hence, the optimisation step of both extraction methods and tissue types play an important role in determining the metabolites that can be recovered from a sample, thus leading to a more thorough metabolomics analysis. However, a complete study to compare both different extraction solvents as well as different tissue types in one single study is still lacking.

The present work thus examines the effects of two extraction parameters on the detection and semi-quantification of primary metabolites in mangosteen. The two different extraction parameters comprised of different solvent ratios of methanol/chloroform/water (3/1/1 v/v) (Cadahía *et al*., 2015) or (2/1/2 v/v) (Lisec *et al*., 2006; De Vos *et al*., 2007). Both parameters are known to be effective for extracting a wide range of metabolites, covering non-polar to polar metabolites. Water and organic solvents (methanol and chloroform) are not only compatible with all analytical platforms including GC-MS, high performance liquid chromatography (HPLC), LC-MS, nuclear magnetic resonance (NMR) and capillary electrophoresis-mass spectrometry (CE-MS), but also facilitate solvent evaporation, produce no salt precipitate and increase the extracted metabolites stability (Lisec *et al*., 2006; Mushtaq *et al*., 2014). More importantly, the influence of these extraction parameters towards the detection and quantification of primary metabolites from different fruit tissues is important to accurately measure the metabolite spatial distribution and provide a better understanding of the fruit's metabolic processes.

Materials and methods

Chemicals and reagents

Analytical grade solvents such as methanol (catalogue number: 106007) and chloroform (catalogue number: 102444) were purchased from Merck (Germany). The derivatisation agents, N, O-bistrifluoroacetamide (BTSFA) (catalogue number: T6381) and methoxyamine hydrochloride (MeOX) (catalogue number: 89803) were purchased from Sigma Aldrich (St. Louis, MO, USA).

Fruit sampling

Mangosteen fruits were collected from Universiti Kebangsaan Malaysia (UKM) mangosteen experimental plots, located at Bangi, Selangor, Malaysia (2°55′09.0″N 101°47′04.8″E) during the months of June-August, 2014. Mangosteen was harvested at week 12 (stage 0, first ripening stage) until week 15 (stage 6, final ripening stage) after anthesis. The colour development of fruit was monitored before the fruit entered the stage 0 and the evaluation was done according to the Mangosteen Maturity Index as reported by Osman and Milan (2006). A total of three fruits were harvested once they reached the dark purple stage (the final stage of mangosteen ripening) (Osman and Milan, 2006). Mangosteen tissues were then separated into pericarp, aril and seed and ground into fine powder using pestle and mortar, to which liquid nitrogen was added, thus ensuring the plant materials remained frozen. The samples were dried using a freeze-dryer to eliminate the water content and kept at -80°C prior to extraction. Three biological replicates of each mangosteen tissue (pericarp, aril and seed) were prepared for each metabolite extraction method.

Metabolite extraction method 1

Method 1 was performed as previously described (Mamat *et al*., 2018b). Mangosteen tissue (200 mg) was extracted with 400 µL of 100% ice-cold chloroform and sonicated in an ultrasonication bath (room temperature, 20 min). Then, the sample was extracted again with a mixture of 1.6 mL of ice-cold distilled water (dH_2O) and methanol (100%) (1/3 v/v) and sonicated again at room temperature for 20 min. The supernatant was obtained after centrifugation (16,100 g, 10 min) and aliquoted into microcentrifuge tubes (50 µL per tube).

Metabolite extraction method 2

Method 2 was performed as previously described (Mamat *et al*., 2018b). Mangosteen tissue (200 mg) was extracted using 3.75 mL of ice-cold

sample extraction solution (100% methanol/100% chloroform/water) (2/1/2 v/v). The sample was immediately vortexed for 10 s and continuously sonicated in an ultrasonication bath at room temperature (40 kHz, 15 min). Then, the mixture was centrifuged for 10 min at maximum speed (16,100 g, room temperature), and the supernatant was aliquoted into microcentrifuge tubes (50 µL per tube).

Sample derivatisation

The supernatant was dried using a vacuum concentrator. Approximately 40 µL of 20 mg/mL MeOX in pyridine and 40 µL of BSTFA were added into each tube of dried supernatant and incubated at 60°C for 1 h.

GC-MS parameter

The sample was analysed using a Perkin Elmer Clarus 600 Turbo Mass GC-MS (Perkin Elmer, USA) coupled to a quadrupole-type MS. The system was operated at 70 eV with helium as the carrier gas. Approximately 1.0 µL of sample was injected into the Elite 5MS (5% diphenyl 95% dimethylpolysiloxane, 30.0 m × 0.25 mm ID × 250 µm) column. Initially, the oven temperature was set at 70°C and increased by 10°C/min to 170°C. The temperature was then increased again by 30°C/min to 280°C and finally held for 3 min. Both injector and transfer temperatures were set to 250°C, while the source temperature was adjusted to 300°C. The full scan range was set to 50-500 m/z and was acquired after 7 min of solvent delay with a split ratio of 20:1.

Data processing and statistical analysis

Raw GC-MS data were obtained from the Turbo Mass software (Perkin Elmer, USA), containing the metabolite name, retention time, match, relative match and peak area. Metabolite identification was performed using NIST (National Institute of Standards and Technology) mass spectral library (2005) with a minimum match of 700. The threshold was a reliable match cut-off for the metabolite identification against NIST library as performed by other studies (Lee *et al*., 2013; Simón-Manso *et al*., 2013). Further analysis was carried out using the AMDIS (Automated Mass Spectral Deconvolution and Identification System) software version 2.71 to extract single metabolite mass spectra from overlapping peaks. Only metabolites present consistently in all three biological replicates of any tissue samples were retained for further analysis. Statistical analysis (two-way ANOVA) was performed using the MetaboAnalyst 3.0 server (www.metaboanalyst.ca). Relative peak area was calculated by dividing the peak area of a particular metabolite with the sum of peak area for the total metabolites times sample weight.

Multivariate data analysis

Processed GC-MS data were normalised to total peak areas, followed by log transformation and pareto scaling prior to multivariate analysis. Pareto scaling was performed to remove systematic differences among variables before a logarithmic transformation to each variable was applied. All data analyses were performed using the MetaboAnalyst 3.0 server (www.metaboanalyst.ca). PCA and PLS-DA analyses were carried out using the SIMCA 14.1 software (Umetrics, Umea, Sweden). PCA and PLS-DA model performance was evaluated using R^2 coefficient to explain the model goodness of fit, and Q^2 for model accuracy. An R^2 value of more than 0.5 and higher than the Q^2 value indicates a good model. To avoid model overfitting, the PLS-DA model was validated using cross validation and permutation testing.

Results

Mangosteen metabolite profiling using GC-MS

Metabolites of mangosteen pericarp, aril and seed were first extracted using two different solvent ratios of methanol/chloroform/water (method 1: 3/1/1 v/v or method 2: 2/1/2 v/v). The samples were then derivatised using BSTFA and run on the GC-MS system, followed by data treatments using several bioinformatics tools (Figure 1). The chromatogram for each mangosteen tissue sample (pericarp, aril and seed) from both extraction methods is not shown. A library search using the AMDIS software against NIST library with the match cut-off of 700 resulted in the putative identification of 43 metabolites (Table 1). 700 is a reliable minimum match value for the identification of metabolites and has been applied in several studies (Lee *et al*., 2013; Simón-Manso *et al*., 2013) to avoid false positive and false negative results (Meyer *et al*., 2010; Grapp *et al*., 2016). The compounds with the match of 700 and above with reliable signals were reported while the compound peaks or compound names with question marks (?) next to them were excluded since they could be a false positive hit. Of the 43 metabolites detected, only 35 known metabolites were statistically significant between methods and/or tissues ($p \leq 0.05$). The metabolites detected were mainly comprised of primary metabolites. Sugars were found to be the most abundant group of metabolites present in the mangosteen fruit, comprising almost half (51%) of the total metabolites detected (calculated based on

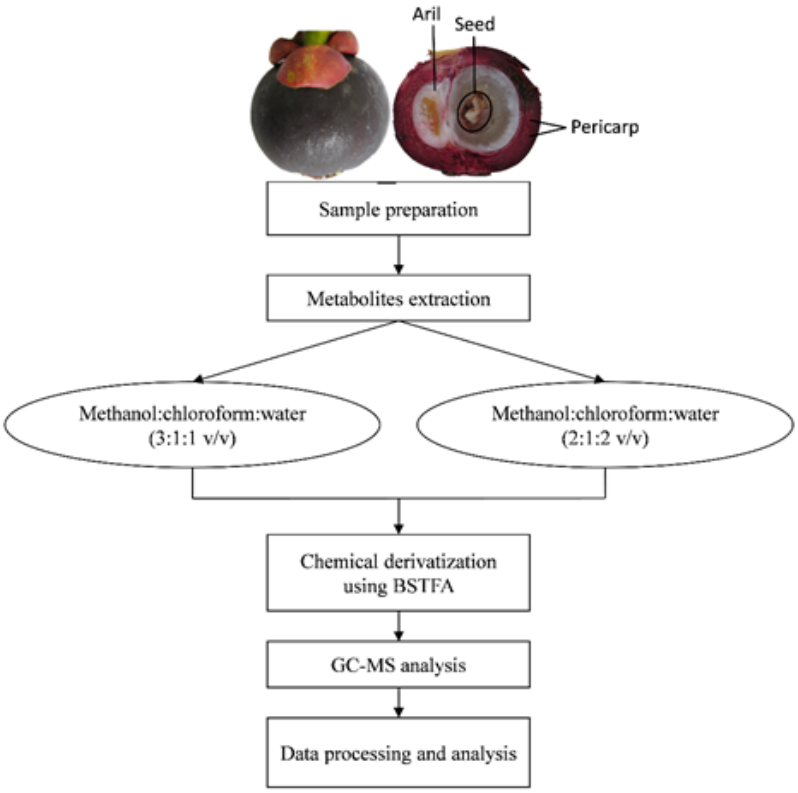

Figure 1. Overview of the methodology.

the number of metabolites detected) and a higher total of relative peak areas as compared to other groups of metabolites for both extraction methods. Meanwhile, 14% of the detected metabolites were organic acids and 12% were sugar acids. Sugar alcohols and alcohols each contributed 5% of the total metabolites while only one aldehyde (butanal, 2%) and one aromatic compound (2H-benopyran, 2%) were detected. Approximately 9% of the detected metabolites were classified as "others" (Table 1) where these metabolites were not categorised into any metabolite class.

Table 1 shows the list of metabolites with their respective relative peak area specific to each extraction method and type of mangosteen tissue where they were detected; either in mangosteen pericarp, aril or seed. For instance, six sugars namely D-fructose, D-glucose, D-ribose, D-xylopyranose, glucopyranose and α-D-glucopyranoside and one organic acid, namely citric acid were detected in all tissues using both methods (Table 1). Other sugars, such as arabinopyranose, were only detected in the mangosteen pericarp, while α-D-galactofuranose only in aril using both extraction methods. Meanwhile, gulose and sorbopyranose were uniquely present from the methanol/chloroform/water 3/1/1 v/v (method 1) whereas arabinofuranose, galacto-hexodialdose, D-xylofuranose, β-D-glucopyranoside and xylulose were found only in the 2/1/2 v/v method (method 2) in either one or two of the three tissues measured. Furthermore, galacturonic acid was consistently detected in the pericarp using both methods while β-D-galactopyranosiduronic acid was only found in the pericarp when extracted using method 1 and galactaric acid using method 2. For organic acids, butanoic acid was found in seed from both extraction methods while propanoic acid was only detected using method 1. Two alcohols namely 2,3-butanediol and threitol were uniquely present from method 1. Thymol-α-D-glucopyranoside was consistently detected in pericarp and aril tissues using both methods while β-hydroxypyruvic acid was consistently present only in the pericarp. Acrylic acid was found only in the seed using method 2.

Multivariate data analysis

Explanatory principal component analysis (PCA) score scatter plot and loading scatter plot (Figures 2a and 2b) were generated to assess the similarities and differences in the metabolites obtained using method 1 and method 2 as well as between different mangosteen tissues. Figure 2a shows a clear separation between the experimental groups giving the best fit model with cumulative X-variance (R^2X) of 0.607 and cross-validated predictive ability (Q^2) of 0.361. Subsequently, supervised PLS-DA was

Table 1. Metabolites from mangosteen fruit pericarp (P), aril (A) and seed (S) extracted using two extraction methods (3/1/1 v/v or 2/1/2 v/v methanol/chloroform/water).

Metabolites	KEGG ID	p value ($p \leq 0.05$)	Method 1			Method 2		
			Methanol/chloroform/water (3/1/1 v/v)			Methanol/chloroform/water (2/1/2 v/v)		
			Relative peak area (average) ± SD			Relative peak area (average) ± SD		
			Pericarp (P)	Aril (A)	Seed (S)	Pericarp (P)	Aril (A)	Seed (S)
Sugars (51%)								
Arabinofuranose	C06115	0.0006	nd	nd	nd	0.1105 ± 0.184	nd	0.0043 ± 0.001
Arabinopyranose	NA	0.0006	0.0769 ± 0.002	nd	nd	0.0711 ± 0.013	nd	nd
D-Fructose	C02336	≥ 0.05	1.8428 ± 0.492	1.2770 ± 0.151	1.8771 ± 0.015	0.8143 ± 0.211	1.6098 ± 0.157	1.2900 ± 0.501
D-Galactose	C00124	≥ 0.05	2.0485 ± 0.905	nd	0.6917 ± 1.081	nd	0.8538 ± 0.529	1.3146 ± 1.245
D-Glucose	C00031	≥ 0.05	0.1405 ± 0.028	0.5120 ± 0.471	2.3935 ± 0.342	0.2980 ± 0.073	0.1640 ± 0.146	0.3779 ± 0.374
D-Ribofuranose	NA	< 0.0001	0.4772 ± 0.114	0.5944 ± 0.226	0.7988 ± 0.431	0.3484 ± 0.190	0.7936 ± 0.296	nd
D-Ribose	C00121	0.0011	0.1380 ± 0.020	0.0300 ± 0.014	0.0140 ± 0.002	0.0593 ± 0.014	0.0170 ± 0.005	0.0080 ± 0.001
D-Xylofuranose	NA	≥ 0.05	nd	nd	nd	nd	0.8638 ± 0.952	0.7535 ± 0.172
D-Xylopyranose	NA	0.0017	0.1125 ± 0.100	0.0181 ± 0.004	0.0092 ± 0.006	0.1383 ± 0.202	0.1108 ± 0.082	0.0037 ± 0.003
D-Xylose	C00181	0.0009	0.0546 ± 0.046	0.1140 ± 0.075	0.0817 ± 0.059	0.0322 ± 0.025	nd	0.0604 ± 0.087
Galacto-hexodialdose	C03269	< 0.0001	nd	nd	nd	0.1292 ± 0.013	nd	nd
Glucopyranose	NA	≥ 0.05	0.8252 ± 0.172	2.0168 ± 0.365	3.0966 ± 1.483	0.6445 ± 0.212	1.3048 ± 0.533	2.2011 ± 1.031
Glycoside	NA	< 0.0001	nd	nd	0.1110 ± 0.159	nd	nd	0.0263 ± 0.011
Gulose	C15923	≥ 0.05	nd	nd	0.2008 ± 0.301	nd	nd	nd
Lyxose	C08348	0.0047	0.0248 ± 0.017	0.0108 ± 0.003	0.0051 ± 0.002	nd	0.0569 ± 0.092	0.0052 ± 0.003
Mannose	C00159	0.0002	0.0880 ± 0.130	0.5682 ± 0.925	0.0472 ± 0.004	0.1315 ± 0.113	nd	0.0386 ± 0.008
Sorbopyranose	NA	< 0.0001	0.0128 ± 0.003	nd	nd	nd	nd	nd
Xylulose	C00310	< 0.0001	nd	nd	nd	0.1355 ± 0.073	nd	0.0006 ± 0.000
α-D-Galactofuranose	NA	0.0051	nd	0.0003 ± 0.000	nd	nd	0.0005 ± 0.000	nd
β-D-Galactofuranose	NA	< 0.0001	nd	nd	0.0651 ± 0.028	nd	0.0789 ± 0.035	0.0374 ± 0.007
α-D-Glucopyranoside	NA	0.0009	3.0484 ± 0.899	7.0709 ± 1.644	5.1506 ± 1.214	2.2319 ± 0.462	4.6907 ± 2.574	4.3413 ± 1.329
β-D-Glucopyranoside	NA	≥ 0.05	nd	nd	nd	0.0002 ± 0.000	nd	nd
Sugar acids (12%)								
Galactaric acid	C00879	< 0.0001	nd	nd	nd	0.0162 ± 0.007	nd	nd
Galacturonic acid	C08348	0.0053	0.0191 ± 0.005	nd	nd	0.0287 ± 0.011	nd	nd
L-Threonic acid	NA	0.0010	nd	nd	0.0190 ± 0.017	nd	nd	0.0072 ± 0.012
Ribonic acid	C01685	< 0.0001	0.0486 ± 0.012	nd	nd	0.022 ± 0.019	0.0001 ± 0.000	nd
β-D-Galactopyranosiduronic acid	NA	< 0.0001	0.0002 ± 0.000	nd	nd	nd	nd	nd

Table 1. (Cont.)

Sugar alcohols (5%)								
Arabinitol	C00532	0.0407	0.0600 ± 0.013	0.0263 ± 0.034	0.0091 ± 0.003	0.0167 ± 0.014	0.0180 ± 0.003	nd
myo-Inositol	C00137	0.0323	0.0383 ± 0.014	nd	0.1996 ± 0.174	0.0168 ± 0.008	0.0051 ± 0.004	0.1686 ± 0.169
Organic acids (14%)								
Arabino-hexaric acid	NA	0.0002	0.0002 ± 0.000	nd	nd	0.0072 ± 0.006	nd	nd
Butanoic acid	C00246	0.0407	nd	nd	0.0265 ± 0.002	nd	nd	0.0154 ± 0.002
Citric acid	C19806	≥ 0.05	0.2564 ± 0.254	0.5022 ± 0.428	0.2380 ± 0.080	0.3682 ± 0.171	0.6249 ± 0.320	0.1515 ± 0.124
L-(+)-Tartaric acid	C00898	< 0.0001	0.0576 ± 0.051	nd	nd	0.0346 ± 0.006	nd	nd
Malic acid	C00149	0.0178	0.2777 ± 0.236	nd	0.6027 ± 0.039	0.1836 ± 0.180	0.0550 ± 0.047	0.1587 ± 0.266
Propanoic acid	C00163	< 0.0001	nd	nd	0.0037 ± 0.001	nd	nd	nd
Alcohols (5%)								
2,3-Butanediol	C00265	< 0.0001	0.0103 ± 0.002	nd	nd	nd	nd	nd
Threitol	C16884	0.0055	nd	nd	0.0020 ± 0.002	nd	nd	nd
Aldehyde (2%)								
Butanal	C01412	0.0021	0.0166 ± 0.003	0.0084 ± 0.012	0.0128 ± 0.015	0.0175 ± 0.003	0.0334 ± 0.022	nd
Aromatic compounds (2%)								
2H-1-Benzopyran	NA	< 0.0001	nd	0.0054 ± 0.002	nd	nd	nd	nd
Others (9%)								
Acrylic acid	C00511	< 0.0001	nd	nd	nd	nd	nd	0.0006 ± 0.000
3,8-Dioxa-2,9-disiladecane	NA	< 0.0001	nd	0.0075 ± 0.005	0.0101 ± 0.000	0.0300 ± 0.010	0.0063 ± 0.000	0.0039 ± 0.002
Thymol-α-D-glucopyranoside	NA	0.0007	0.0278 ± 0.001	0.1265 ± 0.004	nd	0.0218 ± 0.003	0.1607 ± 0.005	nd
β-Hydroxypyruvic acid	C00168	0.0009	0.0458 ± 0.014	nd	nd	0.0384 ± 0.009	nd	nd

Percentage of each metabolite class was calculated as the number of metabolites from each class divided by the total number of putatively identified metabolites (43 metabolites) times 100. Relative peak area was obtained by dividing the peak area of a particular metabolite by the sum of peak area for total metabolites times sample weight. p value represents the statistically significant metabolites either between metabolite extraction methods, or between mangosteen tissues, or the interaction between the metabolite extraction methods and mangosteen tissues obtained from two-way ANOVA test. NA, not available; SD, standard deviation; nd, not detected.

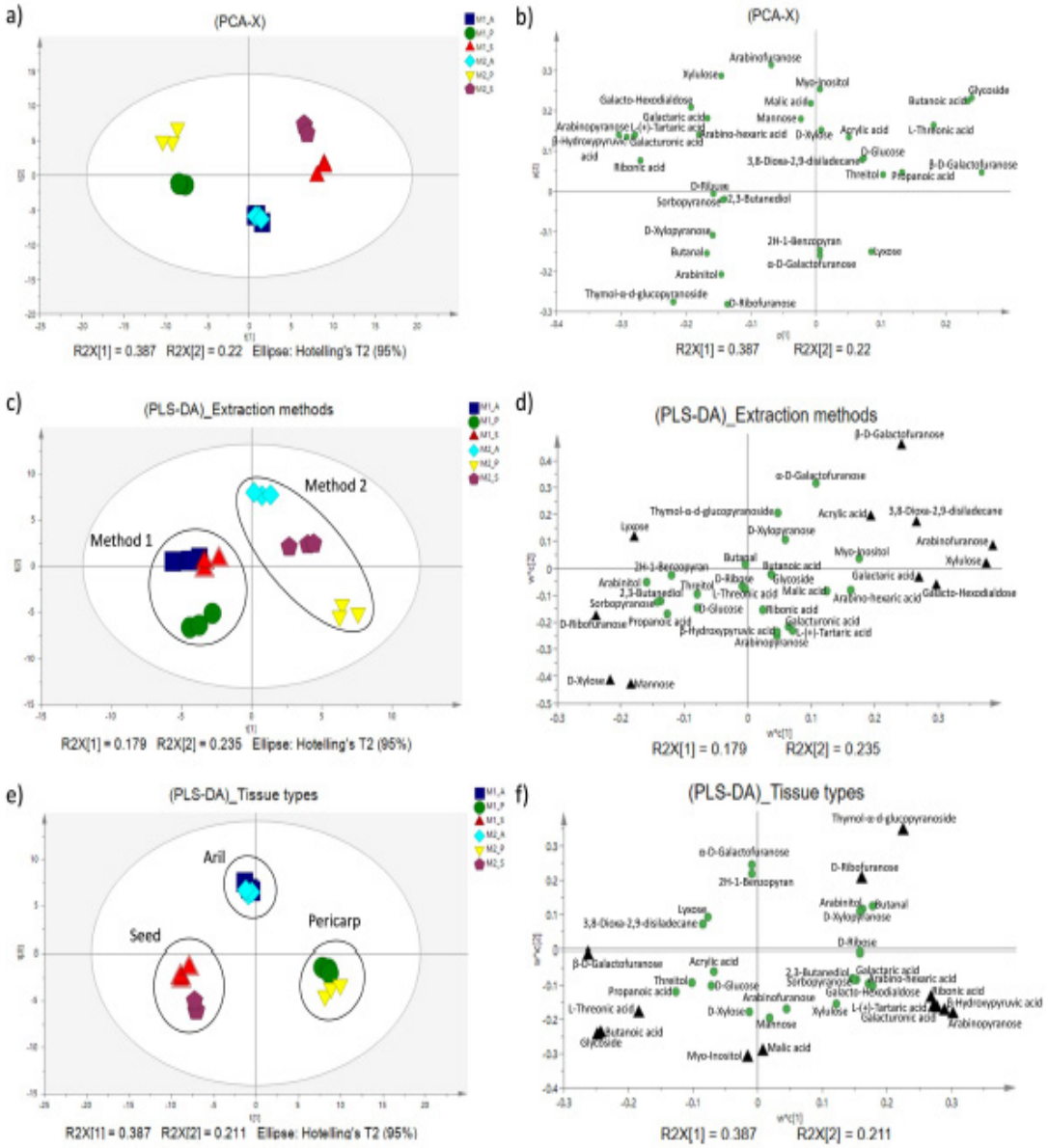

Figure 2. Multivariate analysis; a) PCA score plot, b) PCA loading plot, c) PLS-DA score plot comparing extraction methods, d) PLS-DA loading plot comparing extraction methods showing metabolites with VIP ≥ 1.00 highlighted in black triangle symbols, e) PLS-DA score scatter plot comparing tissue types (pericarp, aril and seed), f) PLS-DA loading plot comparing tissue types showing metabolites with VIP ≥ 1.00 highlighted in black triangle symbols. M1, method 1 (methanol/chloroform/water 3/1/1 v/v); M2, method 2 (methanol/chloroform/water 2/1/2 v/v); P, pericarp; A, aril; S, seed. Each experimental group was represented by three biological replicates (n = 3).

Table 2. Summary of multivariate analysis.

Model	Goodness-of-fit-values				Number of metabolites with VIP ≥1.00
	PCs	R^2X (cum)	R^2Y (cum)	Q^2 (cum)	
PCA	2	0.607	NA	0.361	NA
PLS-DA (extraction methods)	3	0.682	0.966	0.830	11
PLS-DA (tissue types)	2	0.597	0.964	0.939	14

PC, principal component; R^2X (cum), cumulative X-variance; R^2Y (cum), cumulative Y-variance; Q^2 (cum), cumulative cross-validated predictive ability; VIP, variable importance for the projection; NA, not available.

performed to enhance the separation trend found in the PCA. PLS-DA models which were classified according to extraction methods (Figures 2c and 2d) and mangosteen tissue types (Figures 2e and 2f) were obtained and evaluated. A clear separation between the experimental groups was also achieved in the PLS-DA analyses. The R^2X (cum), cumulative Y-variance (R^2Y) and Q^2 value for both PLS-DA models exceeded 50%, thus indicating high variances between experimental groups and that the models were valid (Figure 2, Table 2).

Variable importance for projection (VIP) scores were calculated to determine the influence of each metabolite (Table 2). Metabolites with VIP exceeding 1 (VIP $\geq$ 1.00) can be considered as potential metabolites to discriminate method 1 and method 2 (Azizan *et al*., 2016). For examples, D-ribofuranose, mannose and D-xylose caused the discrimination of samples extracted using method 1, whereas arabinofuranose, xylulose, 3,8-dioxa-2,9-disiladecane, galacto-hexodialdose, acrylic acid and β-D-galactofuranose contributed to the separation of samples obtained from method 2 (Figure 2d). Meanwhile, ribonic acid, arabinopyranose, β-hydroxypyruvic acid, L-(+)-tartaric acid and galacturonic acid caused the separation of mangosteen pericarp from aril and seed as shown in Figure 2f. Thymol-α-D-glucopyranoside and D-ribofuranose contributed to the separation of mangosteen aril whereas the deposition of mangosteen seed at the lower left quadrant of the plot was highly regulated by β-D-galactofuranose, L-threonic acid, butanoic acid, glycoside, malic acid and myo-inositol. PLS-DA models were further validated using the response permutation test and analysis of variance of cross-validated predictive residuals (CV-ANOVA) test (data not shown). The results obtained suggested that all PLS-DA models were highly significant ($p \leq 0.05$).

Discussion

The selection of metabolite extraction method involving extraction solvents and extraction techniques is crucial in determining the type and composition of metabolites that could be extracted from any biological samples (Cevallos-Cevallos *et al*., 2009; Kim and Verpoorte, 2010). The criteria for the selection depend largely on the aims of the study conducted, especially either targeted or non-targeted metabolomics. In this case, a global metabolomics approach was performed using GC-MS analysis to assess the consistency and metabolome coverage between extraction solvents and different mangosteen tissues (Figure 1).

The solvent combination of methanol/chloroform/water was used in the present work due to its ability to extract diverse types of metabolites simultaneously, from polar to non-polar, hydrophilic and hydrophobic molecules (Mushtaq *et al*., 2014). Primary metabolites were mainly detected in the present work with a trace quantity of secondary metabolites. This may be due to the limitation of GC-MS which mostly detects volatile or easily volatilised metabolites such as polar to semi-polar primary metabolites (for example sugars, alcohols, organic acids and amino acids). Instead, LC-MS could be used to detect secondary metabolites as it was reported to be more suitable for the detection of non-volatile, non-derivatised or large compounds such as secondary metabolites (for example flavonoids, alkaloids, saponins and phenylpropanoids (t'Kindt *et al*., 2009; Lee *et al*., 2013).

Explanatory PCA analysis showed a trend of clustering according to fruit tissue types rather than different methods of extraction (Figure 2a). Except for aril sample, pericarp and seed samples did not overlap, indicating differences in their type or level of metabolites. This might be due to the biological nature of each tissue which carries out different structural and metabolic functions. Supervised PLS-DA score plot to preferentially differentiate the effects of different extraction methods and tissue types indicated that the achieved R^2 and Q^2 values for both different extraction methods and tissue types were higher than 50% (Figures 2c and 2e, Table 2), indicating high variance between the experimental groups. Higher precision between tissue types was observed for method 2 as compared to method 1 (Figure 2c). On the other hand, method 2 successfully discriminated pericarp, aril and seed as compared to method 1 (Figure 2c). All three biological replicates in PCA and both of the PLS-DA plots were closely deposited to each other, indicating high reproducibility among the replicates. Response permutation test and CV-ANOVA test were performed to further validate the PLS-DA models. Response permutation test was important to evaluate the risk that the models were specious while CV-ANOVA was used to determine the number of significant components required for the model to avoid overfitting of the model (Eriksson *et al*., 2008; Azizan *et al*., 2012). Results obtained from both validation tests (data not shown) suggested that the PLS-DA models were valid and highly significant, indicating that there were significant differences between the experimental groups (extraction methods and tissue types).

Consistency between two metabolite extraction methods differing in solvent ratios

Some metabolites were successfully extracted from both extraction methods such as sugars including D-fructose, D-glucose, D-xylopyranose and glucopyranose (Table 1), despite using different solvent ratios. Sugar alcohols (myo-inositol and arabinitol), sugar acids (for example ribonic acid and galacturonic acid) and organic acids (for example citric acid and malic acid) were also extracted from both methods in at least one of the mangosteen tissues (Table 1). These compounds are closely related to the ripe condition of the mangosteen fruit. During the onset of fruit ripening, fruit increased its sugar accumulation while reducing its acidity (Osorio *et al*., 2013; Osorio and Fernie, 2014). These biochemical changes occur over time, thus providing the fruit with more desirable traits, making them more appealing to seed dispersal organisms as well as increasing their commercial value. Using method 1 and method 2, sugars were found abundantly in the pericarp, aril and seed, covering more than half of the total metabolites detected with the highest total relative peak areas as compared to other metabolite groups (Table 1). Besides sugars, organic acids, sugar acids and alcohols were also present marginally (2-14%) in various tissues. These metabolites are responsible in determining nutritional quality and postharvest characteristics of a fruit including flavour and aroma (Osorio and Fernie, 2014).

The combination of sugars and their derivative as well as organic acids such as citric, malic and butanoic acids were believed to contribute to the sweetness and acidic taste of mangosteen during the ripening process. Citric and malic acids were reported to be the major organic acids found in most fruits (Osorio and Fernie, 2014). The presence of these metabolites indicates that the TCA cycle was actively regulated in mangosteen during the ripening process. Meanwhile, butanoic acid was reported to be highly responsible for the flavour and smell characteristics in noni fruits (*Morinda citrifolia* L.) (Chan-Blanco *et al*., 2006). However, our study found that this metabolite was exclusively identified from seed tissue, indicating that it might play different roles in seed maturation and hence, demanding further research.

Some metabolites were found to be related to the cell wall degradation and textural softening as well as the protection against biotic or abiotic stress during mangosteen ripening. For example, galacturonic acid was only found in the pericarp sample (Table 1). This is perhaps due to its abundance in pectin, the major polysaccharides in plant primary cell walls and middle lamella (Caffall and Mohnen, 2009; Dettmer *et al*., 2011). Degradation of pectin (pectin breakdown into galacturonic acid) and other plant cell wall polysaccharides (cellulose and hemicelluloses) as well as the dissolution of middle lamella lead to tissue softening and loss of fruit firmness during the ripening process (Goulao and Oliveira, 2008; Osorio and Fernie, 2014). Thymol-α-D-glucopyranoside that was also detected from both extraction methods could be related to the defence activity of mangosteen against plant pathogen attacks as the thymol possesses anti-bacterial (Nabavi *et al*., 2015) and anti-fungal properties (Yang *et al*., 2011).

Variation across metabolites and extraction methods

Even though several compounds discussed earlier were consistently detected in different mangosteen tissues using different extraction methods, several others exhibited different profiles (Table 1). For example, D-fructose was lower in aril as compared to other tissues when method 1 was used but the compound was higher in aril when extracted using method 2. Furthermore, the relative levels of D-galactose, lyxose, mannose, β-D-galactofuranose, butanal and 3,8-dioxa-2,9-disiladecane highly varied when extracted using the two methods (Table 1). This suggests that these compounds were easily influenced by the different solvent ratios and hence should be carefully considered in any subsequent studies.

Furthermore, the degree of solvent polarity may also influence the types of metabolites that could be extracted (Mushtaq *et al*., 2014; Azizan *et al*., 2015). The combination of methanol, chloroform and water solvents were used due to their compatibility and reproducibility in various plant-based metabolomics research (Lisec *et al*., 2006; De Vos *et al*., 2007; Mushtaq *et al*., 2014; Okazaki *et al*., 2016). The use of organic solvents in combination with water is preferable since it could extract diverse types of metabolites simultaneously, from polar to non-polar, hydrophilic and hydrophobic molecules, besides having high compatibility with various metabolomics analytical instruments including GC-MS (Mushtaq *et al*., 2014). In the present work, it was observed that method 2 was inclined to extract more unique polar metabolites in mangosteen tissues than method 1. For example, polar metabolites such as arabinofuranose, galacto-hexodialdose, D-xylofuranose and β-D-glucopyranoside were only detected using method 2. This may be contributed by the higher polar solvent ratios used in this method (two volumes of water as compared to just one in method 1). Moreover, two alcohols (2,3-butanediol and threitol) were exclusively found in method 1 in either pericarp or seed, respectively (Table 1) suggesting the higher

methanol ratio in this method might have contributed to their identification. The results highlighted that the different solvent combinations may increase the detection of certain types of metabolites, signifying the importance of well-optimised extraction procedures in any metabolomics studies.

Conclusion

The present work demonstrated the utilisation of different solvent ratios, 3/1/1 v/v or 2/1/2 v/v of methanol/chloroform/water, to detect primary metabolites in different mangosteen tissues. The results showed that the different solvent ratios affected the metabolite distribution in mangosteen pericarp, aril and seed. Specific localisation of primary metabolites was indicated, which is of high interest for mangosteen fruit ripening and sensory quality research.

Acknowledgement

The present work was financially supported by the UKM Research University (RU) grant (DIP-2018-001), Science Fund grant from the Malaysian Ministry of Science, Technology and Innovation (MOSTI) (02-01-02-SF1237), and Fundamental Research Grant Scheme (FRGS/2/2014/SG05/UKM/02/2) from the Malaysian Ministry of Education (MOE).

References

Aizat, W. M., Jamil, I. N., Ahmad-Hashim, F. H. and Noor, N. M. 2019. Recent updates on metabolite composition and medicinal benefits of mangosteen plant. PeerJ 7: article ID e6324.

Azizan, K. A., Baharum, S. N., Ressom, H. W. and Noor, N. M. 2012. GC-MS analysis and PLS-DA validation of the trimethyl silyl-derivatization techniques. American Journal of Applied Sciences 9(7): 1124-1136.

Azizan, K. A., Ghani, N. H. A. and Nawawi, M. F. 2015. GC-MS based metabolomics and multivariate statistical analysis of Wedelia trilobata extracts for the identification of potential phytochemical properties. Plant OMICS 8(6): 537-543.

Azizan, K. A., Ibrahim, S., Ghani, N. H. A. and Nawawi, M. F. 2016. LC-MS based metabolomics analysis to identify potential allelochemicals in *Wedelia trilobata.* Records of Natural Products 10(6): 788-793.

Cadahía, E., Fernández de Simón, B., Aranda, I., Sanz, M., Sánchez-Gómez, D. and Pinto, E. 2015. Non-targeted metabolomic profile of *Fagus sylvatica* L. leaves using liquid chromatography with mass spectrometry and gas chromatography with mass spectrometry. Phytochemical Analysis 26(2): 171-182.

Caffall, K. H. and Mohnen, D. 2009. The structure, function, and biosynthesis of plant cell wall pectic polysaccharides. Carbohydrate Research 344(14): 1879-1900.

Cevallos-Cevallos, J. M., Reyes-De-Corcuera, J. I., Etxeberria, E., Danyluk, M. D. and Rodrick, G. E. 2009. Metabolomic analysis in food science: a review. Trends in Food Science and Technology 20(11-12): 557-566.

Chaijaroenkul, W., Mubaraki, M. A., Ward, S. A. and Na-Bangchang, K. 2014. Metabolite footprinting of Plasmodium falciparum following exposure to *Garcinia mangostana* Linn. crude extract. Experimental Parasitology 145: 80-86.

Chan-Blanco, Y., Vaillant, F., Perez, A. M., Reynes, M., Brillouet, J.-M. and Brat, P. 2006. The noni fruit (*Morinda citrifolia* L.): a review of agricultural research, nutritional and therapeutic properties. Journal of Food Composition and Analysis 19(6-7): 645-654.

Chen, L. G., Yang, L. L. and Wang, C. C. 2008. Anti-inflammatory activity of mangostins from *Garcinia mangostana*. Food and Chemical Toxicology 46(2): 688-693.

De Vos, R. C., Moco, S., Lommen, A., Keurentjes, J. J., Bino, R. J. and Hall, R. D. 2007. Untargeted large-scale plant metabolomics using liquid chromatography coupled to mass spectrometry. Nature Protocols 2(4): 778-791.

Dettmer, K., Nürnberger, N., Kaspar, H., Gruber, M. A., Almstetter, M. F. and Oefner, P. J. 2011. Metabolite extraction from adherently growing mammalian cells for metabolomics studies: optimization of harvesting and extraction protocols. Analytical and Bioanalytical Chemistry 399(3): 1127-1139.

Eriksson, L., Trygg, J. and Wold, S. 2008. CV-ANOVA for significance testing of PLS and OPLS® models. Journal of Chemometrics 22(11-12): 594-600.

Goulao, L. F. and Oliveira, C. M. 2008. Cell wall modifications during fruit ripening: when a fruit is not the fruit. Trends in Food Science and Technology 19(1): 4-25.

Grapp, M., Maurer, H. H. and Desel, H. 2016. Systematic forensic toxicological analysis by GC-MS in serum using automated mass spectral deconvolution and identification system. Drug Testing and Analysis 8(8): 816-825.

Gullberg, J., Jonsson, P., Nordström, A., Sjöström, M. and Moritz, T. 2004. Design of experiments: an efficient strategy to identify factors influencing extraction and derivatization of *Arabidopsis thaliana* samples in metabolomic studies with gas chromatography/mass spectrometry. Analytical Biochemistry 331(2): 283-295.

Jamil, S. Z. M. R., Rohani, E. R., Baharum, S. N. and Noor, N. M. 2018. Metabolite profiles of callus and cell suspension cultures of mangosteen. 3 Biotech 8(8): article ID 322.

Kim, H. K. and Verpoorte, R. 2010. Sample preparation

for plant metabolomics. Phytochemical Analysis 21(1): 4-13.

Lee, D. K., Yoon, M. H., Kang, Y. P., Yu, J., Park, J. H., Lee, J. and Kwon, S. W. 2013. Comparison of primary and secondary metabolites for suitability to discriminate the origins of Schisandra chinensis by GC/MS and LC/MS. Food Chemistry 141(4): 3931-3937.

Lisec, J., Schauer, N., Kopka, J., Willmitzer, L. and Fernie, A. R. 2006. Gas chromatography mass spectrometry-based metabolite profiling in plants. Nature Protocols 1(1): 387-396.

Mamat, S. F., Azizan, K. A., Baharum, S. N., Noor, N. M. and Aizat, W. M. 2018a. ESI-LC-MS based-metabolomics data of mangosteen (*Garcinia mangostana* Linn.) fruit pericarp, aril and seed at different ripening stages. Data in Brief 17: 1074-1077.

Mamat, S. F., Azizan, K. A., Baharum, S. N., Noor, N. M. and Aizat, W. M. 2018b. Metabolomics analysis of mangosteen (*Garcinia mangostana* Linn.) fruit pericarp using different extraction methods and GC-MS. Plant OMICS 11(2): 89-97.

Matsumoto, K., Akao, Y., Kobayashi, E., Ohguchi, K., Ito, T., Tanaka, T., ... and Nozawa, Y. 2003. Induction of apoptosis by xanthones from mangosteen in human leukemia cell lines. Journal of Natural Products 66(8): 1124-1127.

Meyer, M. R., Peters, F. T. and Maurer, H. H. 2010. Automated mass spectral deconvolution and identification system for GC-MS screening for drugs, poisons, and metabolites in urine. Clinical Chemistry 56(4): 575-584.

Mohamed, G. A., Ibrahim, S. R., Shaaban, M. I. and Ross, S. A. 2014. Mangostanaxanthones I and II, new xanthones from the pericarp of *Garcinia mangostana*. Fitoterapia 98: 215-221.

Mushtaq, M. Y., Choi, Y. H., Verpoorte, R. and Wilson, E. G. 2014. Extraction for metabolomics: access to the metabolome. Phytochemical Analysis 25(4): 291-306.

Nabavi, S. M., Marchese, A., Izadi, M., Curti, V., Daglia, M. and Nabavi, S. F. 2015. Plants belonging to the genus *Thymus* as antibacterial agents: from farm to pharmacy. Food Chemistry 173: 339-347.

Okazaki, K., Kimura, Y., Sugiyama, K., Kami, D., Nakamura, T. and Oka, N. 2016. Discovering metabolic indices for early detection of squash (*Cucurbita maxima*) storage quality using GC–MS-based metabolite profiling. Food Chemistry 196: 1150-1155.

Osman, M. and Milan, A. R. 2006. Fruits for the future 9: Mangosteen-*Garcinia mangostana*. United Kingdom: Southampton Centre for Underutilised Crops.

Osorio, S. and Fernie, A. R. 2014. Fruit ripening: primary metabolism. In Nath, P., Bouzayen, M., Pech, J. C. and Mattoo, A. K. (eds). Fruit Ripening: Physiology, Signalling and Genomics, p. 15-27. United Kingdom: CABI.

Osorio, S., Scossa, F. and Fernie, A. 2013. Molecular regulation of fruit ripening. Frontiers in Plant Science 4: article ID 198.

Parijadi, A. A. R., Putri, S. P., Ridwani, S., Dwivany, F. M. and Fukusaki, E. 2018. Metabolic profiling of *Garcinia mangostana* (mangosteen) based on ripening stages. Journal of Bioscience and Bioengineering 125(2): 238-244.

Shibata, M. A., Iinuma, M., Morimoto, J., Kurose, H., Akamatsu, K., Okuno, Y., ... and Otsuki, Y. 2011. α-Mangostin extracted from the pericarp of the mangosteen (*Garcinia mangostana* Linn.) reduces tumor growth and lymph node metastasis in an immunocompetent xenograft model of metastatic mammary cancer carrying a p53 mutation. BMC Medicine 9: article ID 69.

Simón-Manso, Y., Lowenthal, M. S., Kilpatrick, L. E., Sampson, M. L., Telu, K. H., Rudnick, P. A., ... and Stein, S. E. 2013. Metabolite profiling of a NIST Standard Reference Material for human plasma (SRM 1950): GC-MS, LC-MS, NMR, and clinical laboratory analyses, libraries, and web-based resources. Analytical Chemistry 85(24): 11725-11731.

Sukatta, U., Takenaka, M., Ono, H., Okadome, H., Sotome, I., Nanayama, K., ... and Isobe, S. 2013. Distribution of major xanthones in the pericarp, aril, and yellow gum of mangosteen (*Garcinia mangostana* Linn.) fruit and their contribution to antioxidative activity. Bioscience, Biotechnology, and Biochemistry 77(5): 984-987.

t'Kindt, R., Morreel, K., Deforce, D., Boerjan, W. and Van Bocxlaer, J. 2009. Joint GC–MS and LC–MS platforms for comprehensive plant metabolomics: repeatability and sample pre-treatment. Journal of Chromatography B 877(29): 3572-3580.

Thong, N. M., Quang, D. T., Bui, N. H. T., Dao, D. Q. and Nam, P. C. 2015. Antioxidant properties of xanthones extracted from the pericarp of *Garcinia mangostana* (mangosteen): a theoretical study. Chemical Physics Letters 625: 30-35.

Vondras, A. M., Commisso, M., Guzzo, F. and Deluc, L. G. 2017. Metabolite profiling reveals developmental inequalities in pinot noir berry tissues late in ripening. Frontiers in Plant Science 8: article ID 1108.

Yang, T., Stoopen, G., Yalpani, N., Vervoort, J., de Vos, R., Voster, A., ... and Jongsma, M. A. 2011. Metabolic engineering of geranic acid in maize to achieve fungal resistance is compromised by novel glycosylation patterns. Metabolic Engineering 13(4): 414-425.

Zadernowski, R., Czaplicki, S. and Naczk, M. 2009. Phenolic acid profiles of mangosteen fruits (*Garcinia mangostana*). Food Chemistry 112(3): 685-689.

.